Steel and Composite Structures, *Vol. 31, No. 6 (2019) 617-628*
DOI: https://doi.org/10.12989/scs.2019.31.6.617

Dynamic increase factor for progressive collapse of semi-rigid steel frames with extended endplate connection

Ying Huang [1], Yan Wu [2], Changhong Chen [*2], Zhaohui Huang [3] and Yao Yao [2]

[1] *School of Civil Engineering, Xi'an University of Architecture and Technology, Xi'an, 710055, China*
[2] *School of Mechanical and Civil Engineering, Northwestern Polytechnical University, Xi'an, 710129, China*
[3] *Department of Civil and Environmental Engineering, Brunel University, Uxbridge, Middlesex UB8 3PH, UK*

(*Received January 28, 2019, Revised April 19, 2019, Accepted May 3, 2019*)

Abstract. As an extremely destructive accident, progressive collapse is defined as the spread of an initial local failure from element to element, resulting eventually in the collapse of an entire structure or disproportionately large of it. To prevent the occurrence of it and evaluate the ability of structure resisting progressive collapse, the nonlinear static procedure is usually adopted in the whole structure design process, which considered dynamic effect by utilizing Dynamic Increase Factor (DIF). In current researches, the determining of DIF is performed in full-rigid frame, however, the performance of beam-column connection in the majority of existing frame structures is not full-rigid. In this study, based on the component method proposed by EC3 guideline, the expression of extended endplate connection performance is further derived, and the connection performance is taken into consideration when evaluated the performance of structure resisting progressive collapse by applying the revised plastic P-M hinge. The DIF for structures with extended endplate beam-column connection have been determined and compared with the DIF permitted in current GSA guideline, the necessity of considering connection stiffness in determining the DIF have been proved.

Keywords: Dynamic Increase Factor (DIF); extended endplate connection; the component method; the revised P-M hinge

1. Introduction

Progressive collapse is defined as the spread of an initial local failure from element to element, resulting eventually in the collapse of an entire structure or disproportionately large part of it in ASCE standard 7-10 (2010). In 1968, some load-bearing walls were broken because of a gas explosion in Ronan Point apartment, which resulted in the collapse of one entire corner of the building. This accident drew the attention of researchers to structural progressive collapse issues. In the decades, amount of researches have been conducted to improve the structural progressive collapse resistance. Chen *et al*. (2016a, b) investigated the progressive collapse potential of steel moment framed structures due to abrupt removal of a column based on the energy principle and developed an evaluation method to predict progressive collapse resistance of steel frame structure. Peng *et al*. (2017) investigated the response of flat-plate structures without slab continuous bottom reinforcement under the dynamic removal of an interior column. Yan *et al*. (2018) investigated the performance of the Pinned-Slidable truss joint under progressive collapse scenarios. Rahnavard *et al*. (2018) developed the three dimensional modeling by the finite element method to understand the progressive collapse of high rise buildings with composite steel frames. Yu *et al*. (2018) studied the progressive collapse resistance of reinforced concrete beam-slab substructures by preparing solid-element-based numerical models. Qian and Li (2018) investigated the effects of connection types on the behavior of precast concrete structures to mitigate progressive collapse. Al-Salloum *et al*. (2018) investigated the effectiveness of using bolted steel plates on the behavior of precast beam-column connections under sudden column-loss scenario. Bredean and Botez (2018) evaluated the influence of beam design parameters on the progressive collapse behavir of reinforced concrete structures. Lin *et al*. (2019) proposed a new method for progressive collapse analysis of steel frames under blast load based on the substructure model. Quiel *et al*. (2019) developed and examined experimentally a novel exterior spandrel-to-column moment connection detail for progressive collapse resistant precast concrete building frames. Stephen *et al*. (2019) simulated the sudden column removal in frame buildings and investigated the effect of rising time on the structural response by comparing different alternative numerical approaches. Eren *et al*. (2019) investigated the progressive collapse resistance of infilled RC framed buildings under threat-independent column loss scenarios. Gao (2019) conducted a parametric study to investigate the performance of composite frame under column removal. Fu (2009) simulated the behavior of multi-storey buildings under sudden column removal by building a 3-D finite element model with the ABAQUS package, and proposed that under the same general

*Corresponding author, Associate Professor,
E-mail: changhong.chen@nwpu.edu.cn

ISSN: 1229-9367 (Print), 1598-6233 (Online)

conditions, a column removal at a higher level will induce larger vertical displacement than a column removal at ground level.

ASCE 41 guideline (2013) stipulated that an analysis of the building shall be performed using the linear static procedure (LSP), the linear dynamic procedure (LDP), the nonlinear static procedure (NSP), or the nonlinear dynamic procedure (NDP). In GSA guideline (2003, 2013) and DoD guideline (2013), three analysis procedure are employed: the LSP, the NSP and the NDP, with modifications to accommodate the particular issues associated with progressive collapse. Without considering dynamic effect, geometric nonlinearities and material nonlinearities, the LSP is simplified in structural modelling, however the calculation accuracy is poor. The NDP is capable of giving the most accurate solution, which consuming a lot of time and resource. With accounting for geometric and material nonlinearities, and approximately compensating dynamic effects by using the Dynamic Increased Factor (DIF), the NSP is capable of giving acceptable accurate solution during acceptable period.

Many researches have been conducted to determine the DIF in the nonlinear static procedure. In the previous GSA guideline (2003), a constant Dynamic Increase Factor (DIF) equal to 2.0 is assumed to account for the dynamic effect. However, many researchers (Ruth *et al*. 2006, Mckay 2008) proposed that it is too conservative to consider DIF as 2.0, and Ruth *et al*. (2006) suggested that a DIF of 1.5 is more accurate for a steel moment frame using nonlinear static analysis, while Mckay (2008) proposed a fitting formula of calculating DIF related to the ratio of plastic rotation and yield rotation. In the current GSA guideline (2013), the functions of the allowable plastic rotation and yield rotation are adopted to calculate the DIF of steel frames. To determine the value of DIF accurately, a lot of researches have been done to investigate the effect of various parameters on DIF. Tsai and Lin (2009) built a bilinear elastic-plastic single degree of freedom (SDOF) model to investigate the effect of post-elastic stiffness ratio on DIF, and derived a formula of DIF related to post-elastic stiffness ratio and the ratio of plastic displacement and yield displacement. Instead of considering a SDOF model, Mashhadi and Saffari (2017) recommended an formula related to the post-elastic stiffness ratio and the ratio of plastic rotation and yield rotation by preparing a series of low-rise and mid-rise moment frame structures with different span length and various number of stories.

Instead of relating to the ratio of plastic rotation/ displacement and yield rotation/displacement, some researchers define the DIF as a function of other effective parameters. Liu (2013) proposed a new empirical method to calculate the DIF by defining the DIF as a function of $\max(M_u/M_p)$, which M_u and M_p are the ultimate bending moment under original unamplified static gravity and the plastic moment capacity of an effected beam section respectively. By preparing four tube-type structural models such as framed tube, braced tube, diagrid and hexagrid, Mashhadiali *et al*. (2016) described a recommended methodology for calculating the DIF, and proposed a collapse index to evaluate the progressive collapse potential of tall tube-type buildings. Ferraioli *et al*. (2017) investigated the effect of various design variables on the DIF. Amiri *et al*. (2018) investigated the effect of available structural capacity on DIF value in the reinforced concrete structures and proposed a new empirical DIF formula.

However, most of the above researches are based on structural models with fully rigid beam-to-column connection. Kim and Kim (2009) investigated the progressive collapse performance of steel moment frames with three types of seismic connections, and discovered that the potential of structures which were designed for moderated seismicity occurring progressive collapse varied significantly depending on the connection types. This conclusion indicated that considering connection performance in progressive collapse analysis is necessary.

To account for connection performance in structural progressive collapse analysis, characterizing the relationship between the loads and rotation of the connection is a critical procedure. Many researches have been done to investigate connection performance. Frye and Morris (1975) proposed a polynomial function to express the moment-rotation relationship for all connections of a given type in a standardized non-dimensional form, however, the effects of shear and axial force on connection are ignored, and the material in the members is linear elastic which neglected the effects of strain hardening. Gao *et al*. (2017) conducted a series of experiments to study the behavior of semi-rigid composite joints in structures under column removal, proposed that semi-rigid composite joint possesses good rotation capacity which meets the needs of forming "catenary action" under pure bending moment, and the moment capacity of composite joint decreased linearly along with the increase of tensile force, which indicated the importance of considering axial force in study connection performance. Based on the general principles of the component method suggested in EC3 guidelines (2005), Del Savio *et al*. (2009) proposed a generalized spring mechanical model to estimate the endplate connection behaviour while considering bending moments and axial forces. Stylianidis and Nethercot (2015) further derived explicit expressions of connection performance with considering the effect of bending moment and axial force, applied the expression to a beam-column substructure with flush endplate connection, and validated with available tests (Da Silva *et al*. 2004).

As presented above, the current researches about determining the DIF of structure are mostly based on frame which considering the beam-column joint as rigid connection, and this paper is going to investigate the DIF for the structures with semi-rigid beam-column connection. Because of the good ductility and ability of energy dissipation, extended endplate connections are commonly used in steel frame structures. To determine the DIF for progressive collapse of semi-rigid steel frames with extended endplate connection, in this paper, the generalization of the explicit expression of the relationship between the loads and rotation of the extended endplate connection is further validated based on the joint spring model and the component method. The revised P-M hinge is proposed to describe the relationship between the loads

and rotation of connection and is introduced into the steel frame model to investigate the resisting progressive collapse performance of structural models with extended endplate connection, and the formula of the DIF of semi-rigid steel frames with extended endplate connection have been derived.

2. Expression of joint connection performance

As illustrated in Fig. 1, when the joint is subjected to bending moment and axial force at the beam end, the tension and compression in joint are resisted by bolt rows and column flange respectively. To model the deformational behaviour of the joint accurately, the rotational deformation of the connection, the shear deformation of the column web panel and the beam bending deformation at the beam end should be taken into account. Therefore, the mechanical model of extended endplate connection consists of four zones represented four different kinds of deformation.

The center of compression is located at the mid-thickness of the beam compression flange as suggested in EC3 guidelines (EN 2005). Parameters h_1, h_2 and h_3 represent the distance between the ith rows of bolt and the center of connection compression respectively. h represents the distance between axial force N loading position and the center of connection compression. d is the distance between the connection equivalent tensile location (where rigid link bar KR,t located) and the connection center of compression, analogous to the equivalent lever arm (z_{eq}) employed in EC3 guidelines (EN 2005).

As mentioned above, the deformation behaviour of the joint consists of the rotational deformation of the connection, the shear deformation of the column web panel and the beam bending deformation at the beam end. The rotation composition of joint is shown in Fig. 2, in which φ_b represents the rotation caused by beam bending deformation, θ_1, θ_2 and θ_3 represent the rotation of Rb1,Rb2 and Rb3, caused by the deformation of the tensile components, compressive components and shear components respectively. Therefore the total rotation of joint can be expressed as

$$\varphi = \theta_1 + \theta_2 + \theta_3 + \varphi_b \tag{1}$$

Stylianidis *et al.* (Stylianidis and Nethercot 2015) derived the explicit expression of the relationship between the loads and rotation of the flush endplate connection. To analysis the generalization of the explicit expression, in this paper, the explicit expression of the relationship between

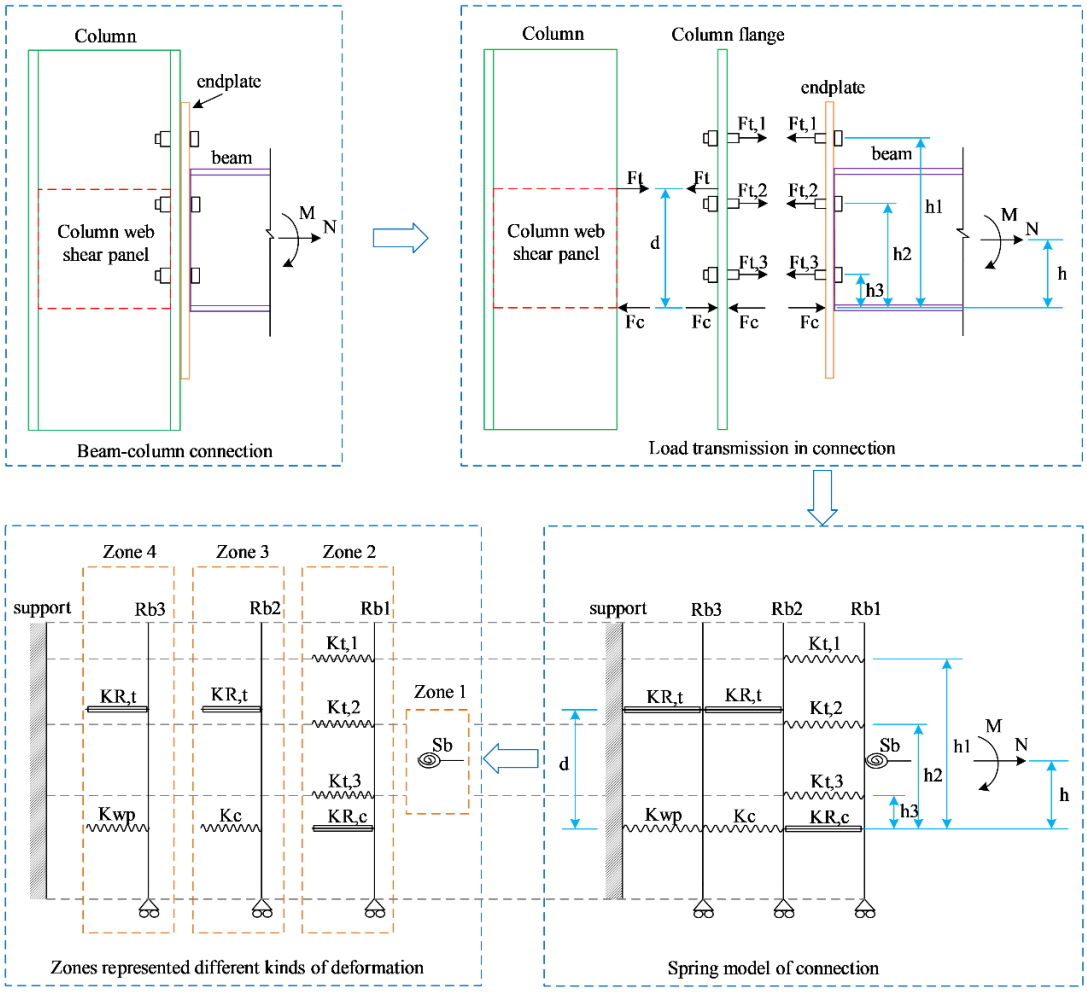

Fig. 1 The mechanical model of extended endplate connection

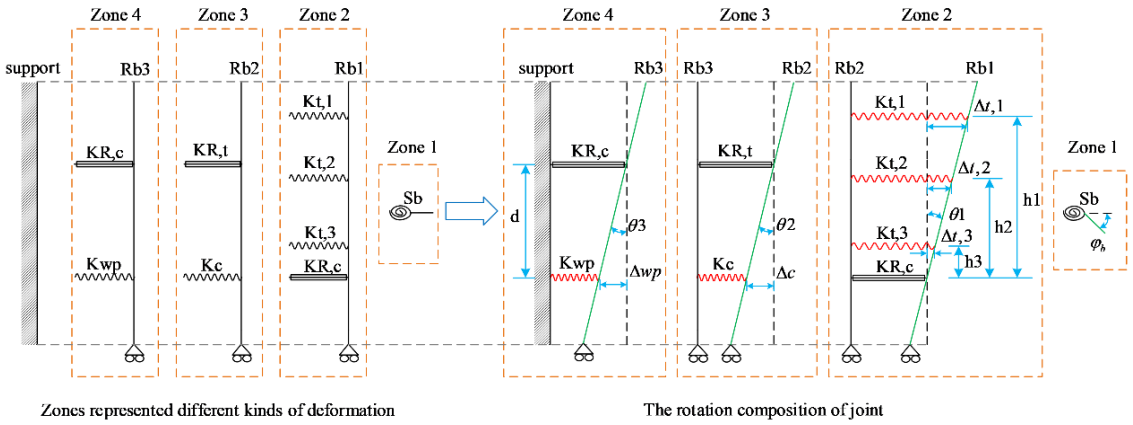

Fig. 2 The rotation composition of connection

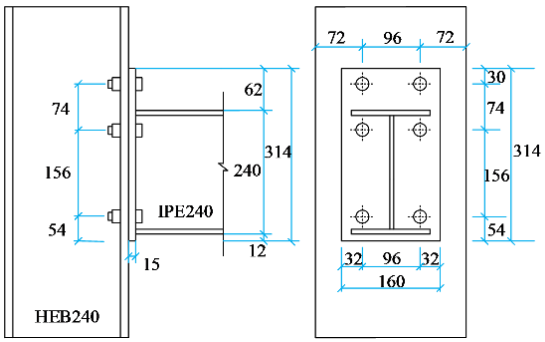

Fig. 3 Extended endplate beam-to-column joint layout

the loads and rotation is further derived and validated with the extended endplate connection.

To further validate the effectiveness of the rotation-load equation of extended endplate connection, comparison and analysis are carried out between the numerical results and experimental results conducted by Lima *et al.* (Lima *et al.* 2002). To be consistent with Lima's (Lima *et al.* 2002) experiment, the beam and column sections are IPE240 and HEB240 respectively, the thickness of the endplate is 15 mm, and the bolts are M20, grade 10.9. The material of beam, column and endplate is S355. The extended endplate beam-to-column joint layout is shown as Fig. 3.

Stylianidis *et al.* (Stylianidis and Nethercot 2015) assumed the connection components may undergo deformation reversal, and simulated the component performance by both a 'loading' and an 'unloading' curve. However, the unloading phase of components are normally not exist in the processes of structures occurring progressive collapse, in this paper, the behaviour of each connection component is characterized by adopting simplified bi-linear relationship as illustrated in Table 1. The yield strength and elastic modulus are same as the experimental datum in Lima's (Lima *et al.* 2002) study. Stylianidis and Nethercot (2015) found that the post-limit responses of the endplate in bending (the weakest component of the bolt-rows), the column web in compression and the column web in shear may be approximated by 0.5%, 1.0% and 1.5% strain-hardening respectively, and the post-limit flexural behaviour of the beam section may be approximated by 1.0%.

Under bending moment M and axial load N, the force analysis of rigid bar 1 is shown as Fig. 4(a). The following equations are drawn from the force equilibrium of rigid bar 1

$$\sum F_{t,i} h_i = M + Nh \tag{2}$$

$$F_c d + N(d-h) = M \tag{3}$$

$$\sum F_{t,i} = N + F_c \tag{4}$$

The expression of calculating F_c is derived by the Eq. (4)

$$F_c = \frac{M - N(d-h)}{d} \tag{5}$$

When the axial load N is less than $M/(d\text{-}h)$ in the Eq. (5), the compressive force in beam bottom flange F_c is greater than 0, and the deformation form of connection tension zone is shown as Fig. 4(b), the rotation of Rb1 θ_1 is

Table 1 Connection components mechanical properties

Specimen		Fy (MPa)	Young's modulus (MPa)	Load-deformation curve
Beam IPE240	Web	363.4	203713	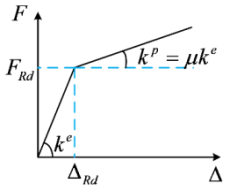
	Flange	340.14	215222	
Column HEB240	Web	372.02	206936	
	flange	342.95	220792	
Endplate	endplate	369.44	200248	

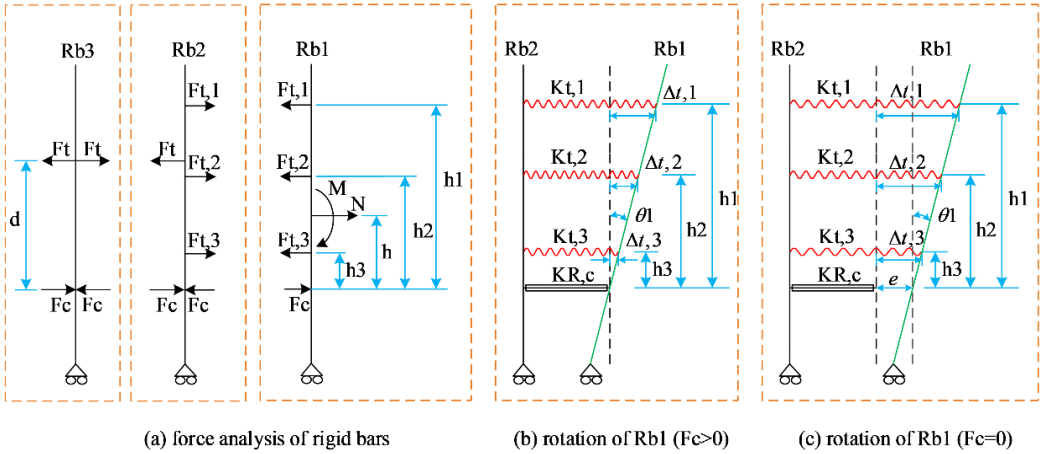

Fig. 4 Force analysis and rotation deformation of Rb1

expressed as follow

$$\theta_1 = \frac{\Delta_{t,i}}{h_i} \tag{6}$$

According to the simplified bi-linear load-deformation relationship shown in Table 1, the following equation can be obtained

$$\Delta = \frac{F - F_{Rd}}{k} + \frac{F_{Rd}}{k^e} \tag{7}$$

where $k = \begin{cases} k^e & F \le F_{Rd} \\ k^p & F > F_{Rd} \end{cases}$.

Substitute the Eqs. (2) and (7) into the Eq. (6), the following equation can be derived

$$\theta_1 = \frac{M + Nh}{A_1} - \frac{A_2}{A_1} \tag{8}$$

where: $A_1 = k_{t,i} h_i^2$, $A_2 = \sum F_{t,Rd,i}\, h_i - \sum F_{t,Rd,i} \frac{k_{t,i}}{k_{t,i}^e} h_i$.

When the axial force N is more than $M/(d\text{-}h)$ in the Eq. (5), the compressive force F_c is equal to 0, namely, there is no contact between endplate and column flange at the beam bottom flange, therefore the rigid bar Rb1 have a axial movement e which is no less than 0. The deformation form of connection tension zone is shown as Fig. 4(c), the rotation of Rb1 θ_1 is expressed as follow

$$\theta_1 = \frac{\Delta_{t,i} - e}{h_i} \tag{9}$$

Substitute the equation $F_c = 0$ into the Eq. (4)

$$\sum F_{t,i} = N \tag{10}$$

Substitute the Eqs. (2), (7) and (10) into the Eq. (9), the following equation can be derived

$$\theta_1 = \frac{M(1 + A_3 X)}{A_1} + \frac{Nh(1 + A_3 \psi)}{A_1} - \frac{A_2 + A_3 \Omega}{A_1} \tag{11}$$

where: $X = \frac{A_3}{A_1 \sum k_{t,i} A_3^2}$

$$\psi = \frac{A_3 - A_1/h}{A_1 \sum k_{t,i} - A_3^2}$$

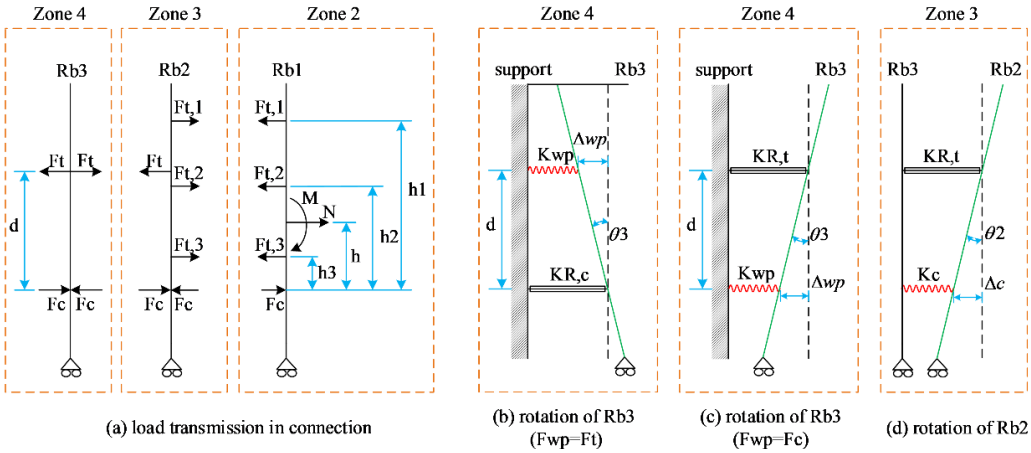

Fig. 5 Load transmission in connection and rotation deformation of Rb2 and Rb3

$$\Omega = \frac{A_2 A_3 - A_1 A_4}{A_1 \sum k_{t,i} - A_3^2}$$

$$A_1 = \sum k_{t,i} - h_i^2$$

$$A_2 = \sum F_{t,Rd,i} - h_i \ - \sum F_{t,Rd,i} \frac{k_{t,i}}{k_{t,i}^e} h_i$$

$$A_3 = \sum k_{t,i} - h_i$$

$$A_4 = \sum F_{t,Rd,i} - \sum F_{t,Rd,i} \frac{k_{t,i}}{k_{t,i}^e}$$

Seen from Fig. 5(d), the rotation of Rb2 caused by deformation of connection compression component can be expressed as follow

$$\theta_2 = \frac{\Delta_c}{d} \tag{12}$$

Substitute the Eq. (5) and (7) into the Eq. (12), the following equation can be derived

$$\theta_2 = \frac{M}{B_1} + \frac{Nh(1-d/h)}{B_1} - B_2 \tag{13}$$

where: $B_1 = k_c d^2$, $B_2 = \frac{F_{c,Rd}}{d}\left(\frac{1}{k_c} - \frac{1}{k_c^e}\right)$

Under bending moment M and axial force N, the load transmission in connection is shown as Fig. 5(a). The following equations are drawn from the force equilibrium of rigid bar 3

$$F_c = \frac{M - N(d-h)}{d} = \frac{M + Nh}{d} - N \tag{14}$$

$$F_t = \frac{M + Nh}{d} \tag{15}$$

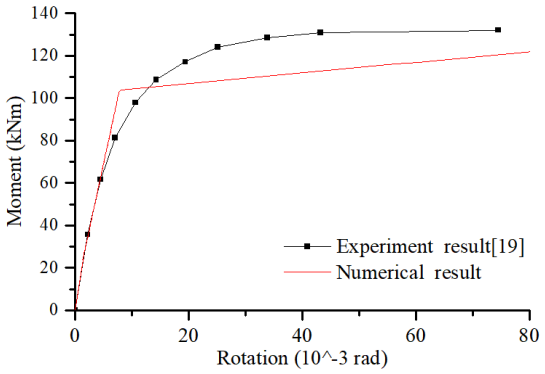

(a) N = -15%

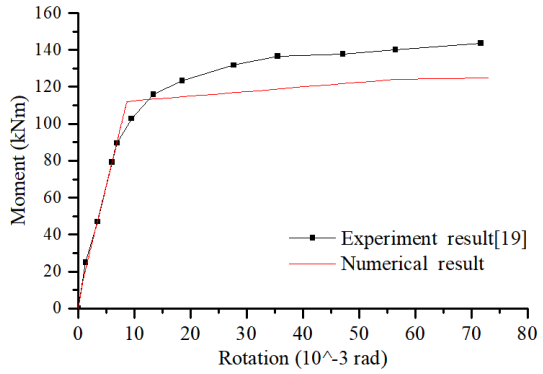

(b) N = -10%

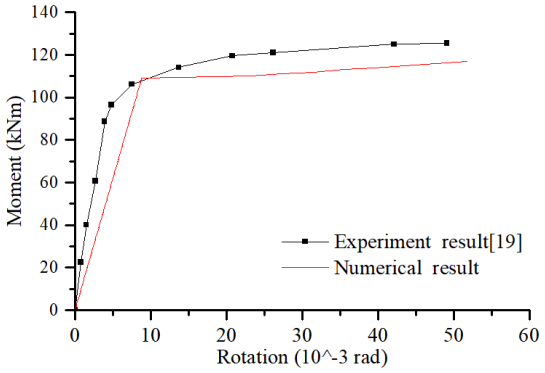

(c) N = 0%

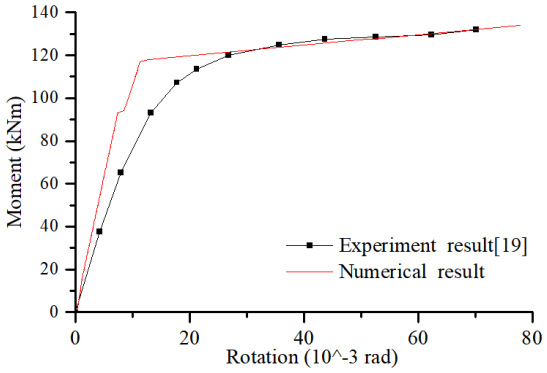

(d) N = +10%

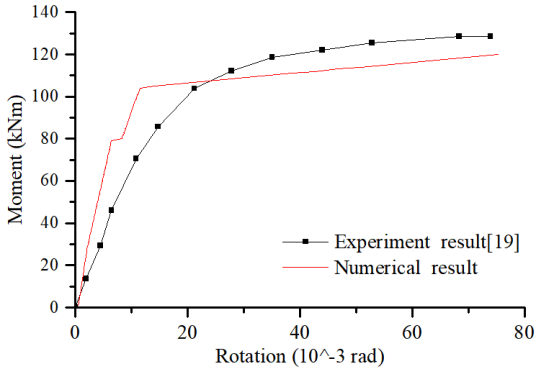

(e) N = +20%

Fig. 6 Connection rotation-moment predictions

The column web in connection is subjected to tensile internal force F_t and compressive internal force F_c, therefore, the column web shear force F_{wp} is equal to the minimum between the connection tensile and compressive force.

$$F_{wp} = \begin{cases} F_c = (M + Nh)/d - N & N > 0 \\ F_t = (M + Nh)/d & N \le 0 \end{cases} \tag{16}$$

The rotation of Rb3 caused by column web shear deformation can be expressed as

$$\theta_3 = \frac{\Delta_{wp}}{d} \tag{17}$$

Substitute the Eqs. (16) and (7) into the Eq. (17), the following equation can be derived

$$\theta_3 = \frac{M}{C_1} + \frac{NhC_3}{C_1} - C_2 \tag{18}$$

where: $C_1 = k_{wp} d^2$, $C_2 = \frac{F_{wp,Rd}}{d}\left(\frac{1}{k_{wp}} - \frac{1}{k_{wp}^e}\right)$, $C_3 = \begin{cases} 1 - \frac{d}{h} & N > 0 \\ 1 & N \le 0 \end{cases}$

Adopting the analytical formula given in EC3 guidelines (EN 2005), the prediction of the elastic stiffness (k^e), design resistance (F_{Rd}) and post-limit stiffness (k^p) of the basic connection components are shown as Table 2.

Considering the beam as a cantilever beam under axial force N and bending moment M, the effect of axial force N can be ignored because of N have limited contribution to beam bending deformation. Based on the elastic beam theory, the rotation at the beam end caused by beam bending deformation can be expressed as

$$\varphi_b = \frac{ML}{3EI_b} \tag{19}$$

Substituting the mechanical properties of connection components in Table 2 into the Eqs. (11), (13) and (18), and applying the bending moment (M) increased by 1*kNm*, with the axial load (N) remains -15%, -10%, 10% and 20% of the design plastic resistance $N_{pl,Rd}$ of its cross-section, the rotation-moment curves are obtained and compared with Lima's (Lima *et al*. 2002) experiment results

Seen from Fig. 6, the numerical results obtained by formula calculation are basically consistent with Lima's (Lima *et al*. 2002) experiment results, and the effectiveness of the Eq. (1) is further validated.

3. Determination of the dynamic increase factor

To accurately determine the DIF of semi-rigid steel frame structures with considering connection stiffness, as shown in Fig. 7, a five-story and four-span planar structure model in SAP2000 software is employed. The section of beam and column in this model are IPE240 and HEB240 respectively, and the material of all components are S355. Both material yield and connection stiffness are considered in this model by introducing M hinge and the revised P-M hinge respectively.

Material failure is not considered in the determination of connection performance, to be consistent in material property of the whole structural frame, characterize the behaviour of structure component by adopting simplified bi-linear approximations as illustrated in Fig. 8. The yield moment M_y and the yield rotation θ_y are taken as permitted in FEMA356 ((FEMA) Federal Emergency Management Agency 2000), and the strain-hardening slope can be taken

Table 2 The mechanical properties of connection components

Component	F_{Rd} (kN)	k^e (kN/mm)	k^p (kN/mm)
Bolt-row 1	274.5	536.6	18.46
Bolt-row 2	267.7	500.19	13.08
Bolt-row3	325.8	651.8	12.42
Column web in compression	654.3	2152.1	21.52
Column web in shear	642.5	1175.4	17.63

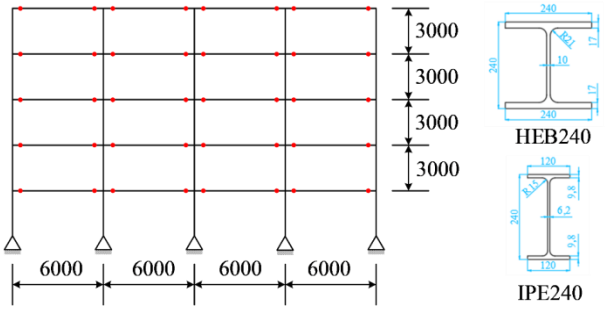

Fig. 7 Structure models schematic

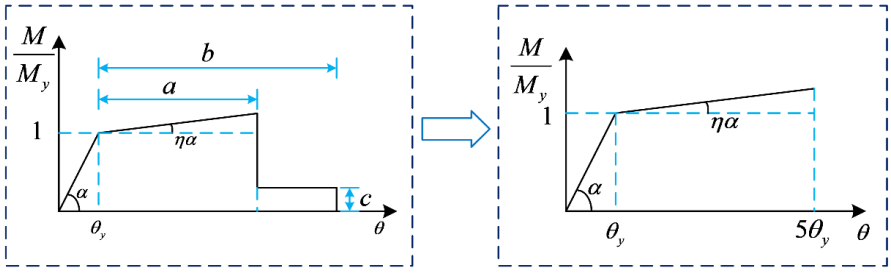

Fig. 8 The simplified bi-linear material property

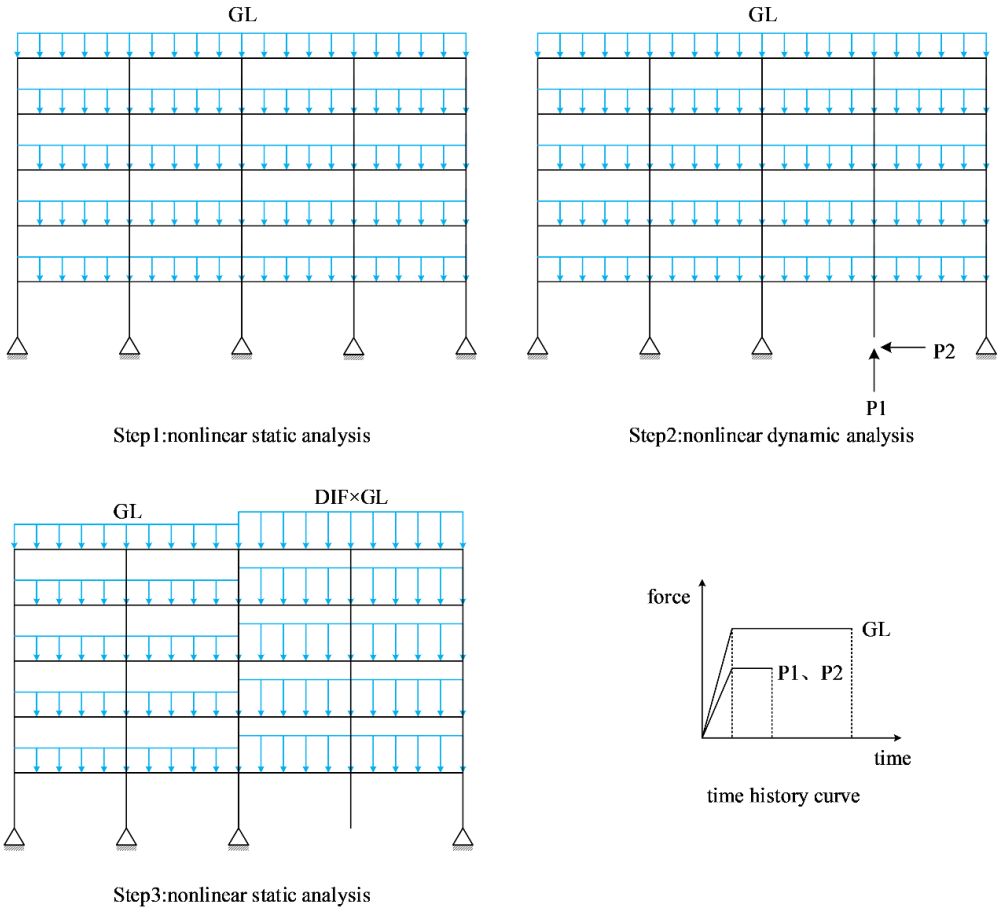

Fig. 9 The procedure of determining DIF

as 3% of the elastic slope as FEMA356 ((FEMA) Federal Emergency Management Agency 2000) suggested, without considering material failure. The material nonlinearity is considered by modeling concentrated plastic hinge in structure model.

Characterizing the connection rotation-moment relationship with the mechanical equation proposed in section 2, and the maximum rotation acceptance criteria of bolted endplate connection is 0.035rad in ASCE41 (ASCE 2013), however, Yang (Yang and Tan 2012) proposed that the acceptance criteria of rotation capacities suggested in ASCE41 (ASCE 2013) for steel connections are too conservative. In this study, the limit joint rotation is taken 0.15rad as suggested in Yang's (Yang and Tan 2012) conclusion.

As illustrated in section 2, joint connection rotation is related to bending moment and axial force, the revised P-M hinge is proposed to introduce connection stiffness into structure model. Increasing the value of axial force from -150KN up to +350KN with increment of 10KN, the corresponding 51 sets of connection rotation-moment curve can be obtained respectively. Enter the axial force value and the corresponding rotation-moment curve into the rotation-moment data of P-M hinge, and in which assume the yield moment is the same when the axial force changed.

Two kinds of hinges (M hinge and P-M hinge) are introduced into structure model, and the accuracy DIF expression of structures which considered connection stiffness have been determined. The procedure of determining the DIF is shown as Fig. 9:

(1) Apply the uniform load GL into structure, and perform nonlinear static analysis to obtain the reaction forces of the column-removed location;
(2) Apply the reaction force at the column-removed location and the uniform load GL, perform nonlinear dynamic analysis, and the maximum ratio of θ_{max}/θ_y among all the beams of the bays effected by the column removal location is obtained;
(3) Apply the uniform load DIF×GL into the beams which adjacent to the removed column location, apply GL into the remainder of beams, and perform nonlinear static analysis;
(4) The ratio of θ_{max}/θ_y is obtained and compared with the ratio obtained in step2;
(5) Modify the DIF and rerun the model until the maximum ratio of θ_{max}/θ_y is same as the ratio obtained in step 2.

By removing the column of different location and applying different value of load, a series of numerical results are obtained, the deformed shape of models removed column are shown in Fig. 10. As explained before, the revised P-M hinge and M hinge represent connection stiffness and material nonlinear property respectively, in the

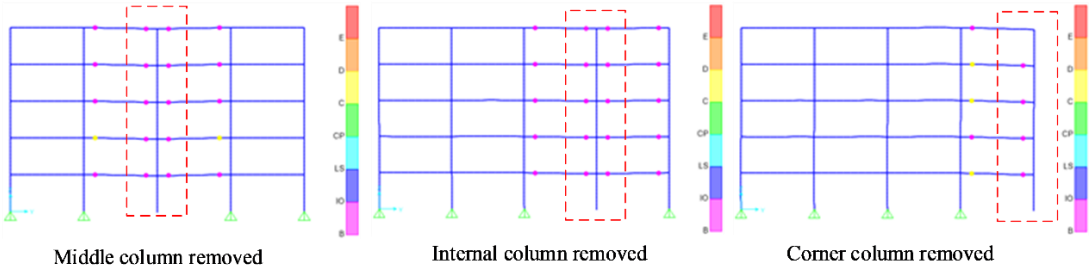

(a) Deformed steel frame model with P-M hinge occuring

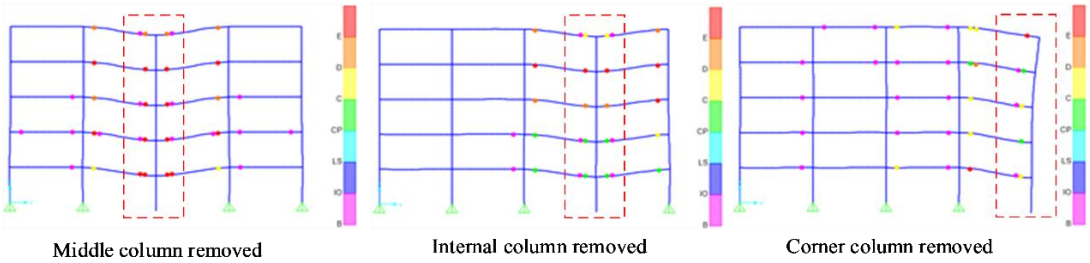

(b) Deformed steel frame model with both P-M hinge and M hinge occuring

Fig. 10 The deformed shape model

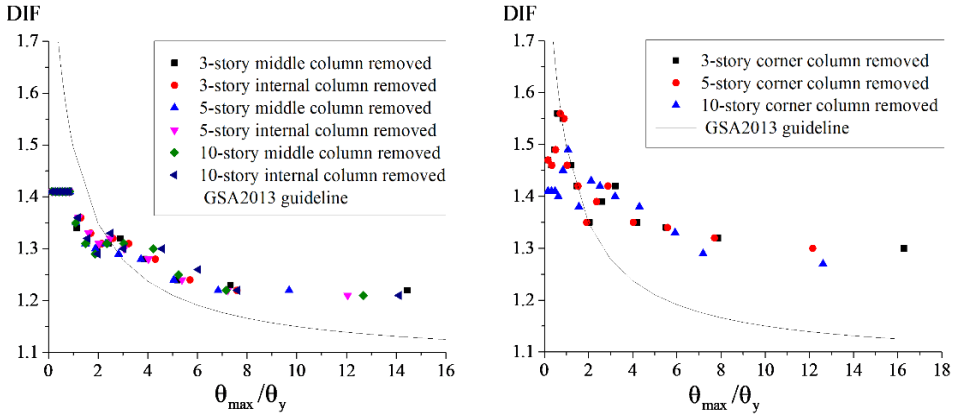

Fig. 11 Comparison of DIF as a function of normal rotation

definition of the revised P-M hinge, each specific value of axial force N exists a corresponding bending moment–rotation curve, with the increasing of load applied into the model, the P-M hinges occurred in the beams which adjacent to the column-removed location, which indicates the connection reached yield bending moment and yield rotation firstly, and no hinge occurred in the beams which is not effected by removed column, When the load applied into the structure further increased, the M hinge began to occur in the beams which adjacent to the column-removed location, which indicates that connection reached yield rotation before the beam material yield, and when the function of DIF is related to the rotation of beam, it is necessary to consider semi-rigid connection stiffness into the determination of DIF.

Comparison of DIF as a function of normal rotation θ_{max}/θ_y for different models with different column-removed location is shown in Fig. 11. The following conclusions can be drawn:

- When $\theta_{\max}/\theta_y$<1, the structure remains elastic, the development law of DIF for corner column removed is gradually increasing with $\theta_{\max}/\theta_y$ increasing, and the DIF basically remain the same for internal column removed;
- The DIF obtained from numerical analysis which considering connection stiffness is different from the DIF permitted in current guideline;
- When the $\theta_{\max}/\theta_y$ < 2~3, the DIF permitted in current guideline is too conservative, and when $\theta_{\max}/\theta_y$ > 2~3, the DIF permitted in current guideline is smaller than the numerical result, which indicates that this DIF is less secure.

As illustrated in Fig. 12, the relationship curves of DIF and normal rotation $\theta_{\max}/\theta_y$ are divided into two parts:

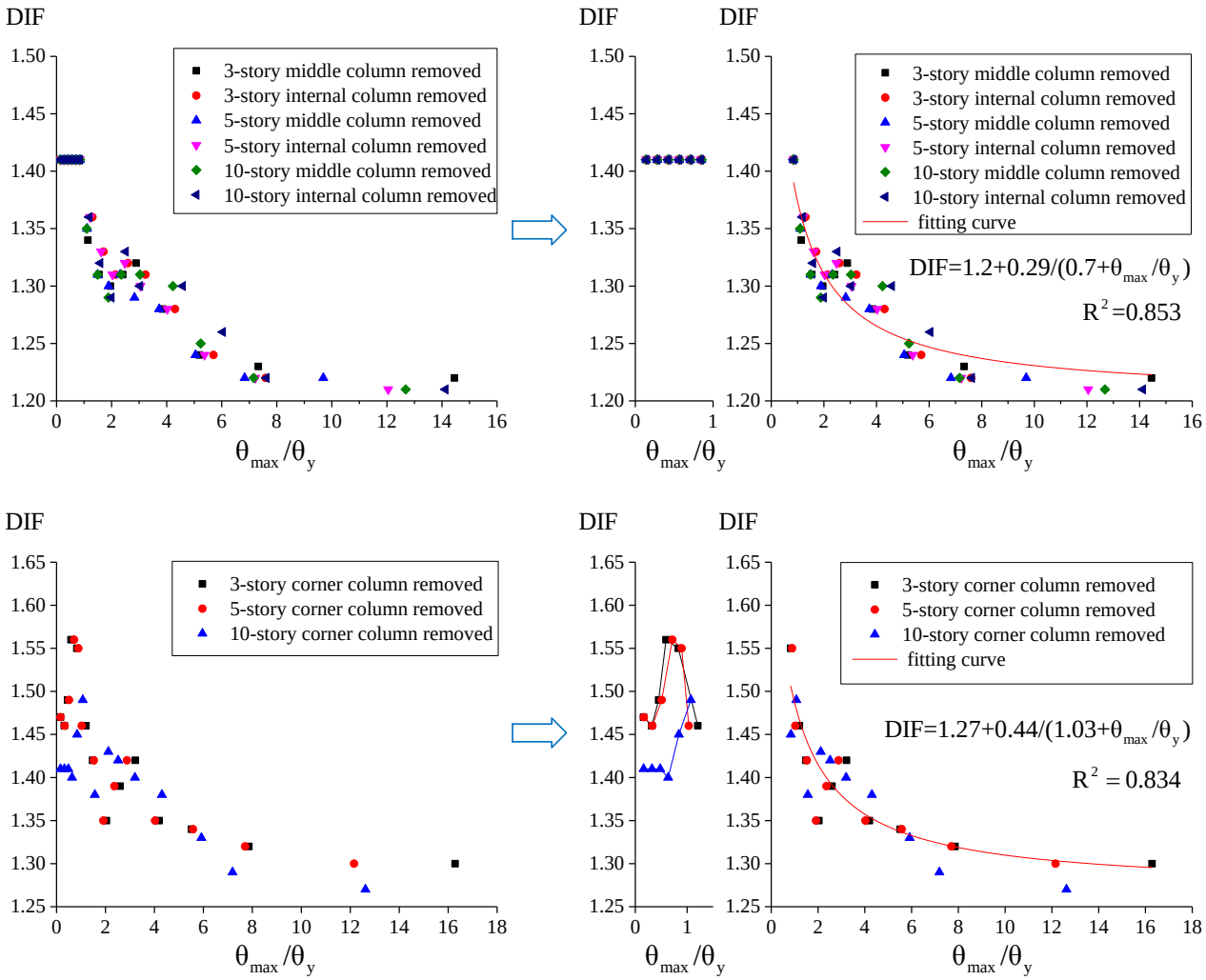

Fig. 12 Curve fitting of DIF about normal rotation θ_{max}/θ_y

- When $\theta_{\max}/\theta_y$ <1 (i.e., the structure remains elastic), the development law of DIF for corner column removed is gradually increasing with $\theta_{\max}/\theta_y$ increasing, and the DIF basically remain the same for internal column removed;
- When $\theta_{\max}/\theta_y \geq 1$, the relationship between DIF and normal rotation $\theta_{\max}/\theta_y$ can be described by the following formulas:

when the internal column was removed:

$$DIF = 1.2 + \frac{0.29}{0.7+\theta_{\max}/\theta_y} \quad (R^2 = 0.853)$$

when the corner column was removed:

$$DIF = 1.27 + \frac{0.44}{1.03+\theta_{\max}/\theta_y} \quad (R^2 = 0.834)$$

In this section, the DIF for steel frame structures with extended endplate connection is determined and compared with the DIF permitted in current guideline. It is found that when the $\theta_{\max}/\theta_y$ is small, the DIF permitted in current guideline which did not consider connection performance is too conservative, and when the $\theta_{\max}/\theta_y$ becoming larger, the value of DIF permitted in current guideline which did not consider connection performance is less secure, which indicates that it is necessary and feasible to consider the connection performance in determining the DIF in real structure design.

4. Conclusions

This paper investigated the progressive collapse performance of structural models with extended endplate connection, and verify the necessity and feasibility of considering the connection performance in determining the DIF in real structure design. In this study, the explicit expression of the relationship between the loads and rotation of the extended endplate connection is further derived based on the joint spring model and the component method. The revised P-M hinge is proposed to describe the relationship between the loads and rotation of connection and is introduced into the steel frame model. The DIF obtained from steel frame structures with extended endplate connection is compared with the DIF permitted in current

guideline, and the result show that when the $\theta_{\max}/\theta_y$ is small, the DIF permitted in current guideline which did not consider connection performance is too conservative, and when the $\theta_{\max}/\theta_y$ becoming larger, the value of DIF permitted in current guideline which did not consider connection performance is less secure, and the nonlinear fitting formulas for determining the DIF of semi-rigid steel frame structures with considering connection stiffness are derived.

Acknowledgments

The authors would like to acknowledge the financially supported by the National Natural Science Foundation of China (51408489, 51248007, 51308448, 51301136 and 51508464), the Shanxi National Science Foundation of China (2017JQ7255), China Scholarship Council and the Fundamental Research Funds for the Central Universities (3102014JCQ01047).

References

Al-Salloum, Y.A., Alrubaidi, M.A., Elsanadedy, H.M., Almusallam, T.H. and Iqbal, R.A. (2018), "Strengthening of precast RC beam-column connections for progressive collapse mitigation using bolted steel plates", *Eng. Struct.*, **161**, 146-160.

Amiri, S., Saffari, H. and Mashhadi, J. (2018), "Assessment of dynamic increase factor for progressive collapse analysis of RC structures", *Eng. Fail. Anal.*, **84**, 300-310.

ASCE (2010), Minimum Design Loads for Buildings and Other Structures, Reston, VA, USA.

ASCE (2013), Seismic Evaluation and Retrofit of Existing Buildings, ASCE/SEI 41-13, Reston, VA, USA.

Bredean, L.A. and Botez, M.D. (2018), "The influence of beams design and the slabs effect on the progressive collapse resisting mechanisms development for RC framed structures", *Eng. Fail. Anal.*, **91** 527-542.

Chen, C.H., Zhu, Y.F., Yao, Y. and Huang, Y. (2016a), "Progressive collapse analysis of steel frame structure based on the energy principle", *Steel Compos. Struct., Int. J.*, **21**(3), 553-571. http://dx.doi.org/10.12989/scs.2018.28.2.233

Chen, C.H., Zhu, Y.F., Yao, Y., Huang, Y. and Long, X. (2016b), "An evaluation method to predict progressive collapse resistance of steel frame structures", *J. Constr. Steel. Res.*, **122**, 238-250.

Da Silva, L.S., de Lima, L.R., Da SVellasco, P. and de Andrade, S.A. (2004), "Behaviour of flush end-plate beam-to-column joints under bending and axial force", *Steel Compos. Struct.*, **4**(2), 77-94.

Del Savio, A.A., Nethercot, D.A., Vellasco, P.D.S., Andrade, S. and Martha, L.F. (2009), "Generalised component-based model for beam-to-column connections including axial versus moment interaction", *J. Constr. Steel. Res.*, **65**(8-9), 1876-1895.

Department of Defense (DoD) (2013), DESIGN OF BUILDINGS TO RESIST PROGRESSIVE COLLAPSE, Unified Facilities Criteria.

EN, E.C.F.S. (2005), Design of steel structures, part 1-8: Design of joints, Eurocode 3.

Eren, N., Brunesi, E. and Nascimbene, R. (2019), "Influence of masonry infills on the progressive collapse resistance of reinforced concrete framed buildings", *Eng. Struct.*, **178**, 375-394.

Federal Emergency Management Agency (2000), FEMA356, Prestandard and Commentary for the Seismic Rehabilitation of Buildings, Washington, D.C., USA.

Ferraioli, M., Lavino, A. and Mandara, A. (2017), "06.03: Dynamic increase factor for nonlinear static alternate path analysis of steel moment-resisting frames against progressive collapse", *ce/papers.*, **1**(2-3), 1437-1446.

Frye, M.J. and Morris, G.A. (1975), "Analysis of flexibly connected steel frames", *Can. J. Civil Eng.*, **2**(3), 280-291.

Fu, F. (2009), "Progressive collapse analysis of high-rise building with 3-D finite element modeling method", *J. Constr. Steel Res.*, **65**(6), 1269-1278.

Gao, S. (2019), "Nonlinear finite element failure analysis of bolted steel-concrete composite frame under column-loss", *J. Constr. Steel. Res.*, **155**, 62-76.

Gao, S., Guo, L., Fu, F. and Zhang, S. (2017), "Capacity of semi-rigid composite joints in accommodating column loss", *J. Constr. Steel Res.*, **139**, 288-301.

GSA, U.S. (2003), "Progressive collapse analysis and design guidelines for new federal office buildings and major modernization projects", Washington, D.C., USA.

GSA, U.S. (2013), "Progressive collapse analysis and design guidelines for new federal office buildings and major modernization projects", Washington, D.C., USA.

Kim, T. and Kim, J. (2009), "Collapse analysis of steel moment frames with various seismic connections", *J. Constr. Steel. Res.*, **65**(6), 1316-1322.

Lima, L.R.O.D., Silva, L.S.D., Da, S., Vellasco, P.C.G. and Andrade, S.A.L.D. (2002), "Experimental analysis of extended end-plate beam-to-column joints under bending and axial force", *Eurosteel Coimbra*, 1121-1130.

Lin, S., Yang, B., Kang, S. and Xu, S. (2019), "A new method for progressive collapse analysis of steel frames", *J. Constr. Steel. Res.*, **153**, 71-84.

Liu, M. (2013), "A new dynamic increase factor for nonlinear static alternate path analysis of building frames against progressive collapse", *Eng. Struct.*, **48**, 666-673.

Mashhadi, J. and Saffari, H. (2017), "Effects of Postelastic Stiffness Ratio on Dynamic Increase Factor in Progressive Collapse", *J. Perform. Constr. Fac.*, **31**(6), 4017107.

Mashhadiali, N., Kheyroddin, A. and Zahiri-Hashemi, R. (2016), "Dynamic Increase Factor for Investigation of Progressive Collapse Potential in Tall Tube-Type Buildings", *J. Perform. Constr. Fac.*, **30**(6), 4016050.

Mckay, A.E. (2008), "Alternate Path method in progressive collapse analysis: Variation of dynamic and non-linear load increase factors", *Pract. Period. Struct. Des. Const.*, **17**(4), 152-160.

Peng, Z., Orton, S.L., Liu, J. and Tian, Y. (2017), "Experimental Study of Dynamic Progressive Collapse in Flat-Plate Buildings Subjected to Exterior Column Removal", *J. Struct. Eng.*, **143**(9), p. 04017125.

Qian, K. and Li, B. (2018), "Performance of Precast Concrete Substructures with Dry Connections to Resist Progressive Collapse", *J. Perform. Constr. Fac.*, **32**(2), 4018005.

Quiel, S.E., Naito, C.J. and Fallon, C.T. (2019), "A non-emulative moment connection for progressive collapse resistance in precast concrete building frames", *Eng. Struct.*, **179**, 174-188.

Rahnavard, R., Fard, F.F.Z., Hosseini, A. and Suleiman, M. (2018), "Nonlinear Analysis on Progressive Collapse of Tall Steel Composite Buildings", *Case Stud. Const. Materials.*, **8**, S1390319133.

Ruth, P., Marchand, K.A. and Williamson, E.B. (2006), "Static equivalency in progressive collapse alternate path analysis: Reducing conservatism while retaining structural integrity", *J. Perform. Constr. Fac.*, **20**(4), 349-364.

Stephen, D., Lam, D., Forth, J., Ye, J. and Tsavdaridis, K.D. (2019), "An evaluation of modelling approaches and column

removal time on progressive collapse of building", *J. Constr. Steel. Res.*, **153**, 243-253.
Stylianidis, P.M. and Nethercot, D.A. (2015), "Modelling of connection behaviour for progressive collapse analysis", *J. Constr. Steel. Res.*, **113**, 169-184.
Tsai, M. and Lin, B. (2009), "Dynamic amplification factor for progressive collapse resistance analysis of an RC building", *Struct. Des. Tall Spec. Build.*, **18**(5), 539-557.
Yan, S., Zhao, X., Chen, Y., Xu, Z. and Lu, Y. (2018), "A new type of truss joint for prevention of progressive collapse", *Eng. Struct.*, **167**, 203-213.
Yang, B. and Tan, K.H. (2012), "Numerical analyses of steel beam–column joints subjected to catenary action", *J. Constr. Steel. Res.*, **70**, 1-11.
Yu, J., Luo, L. and Yi, L. (2018), "Numerical study of progressive collapse resistance of RC beam-slab substructures under perimeter column removal scenarios", *Eng. Struct.*, **159**, 14-27.

DL